CLEAN RESOURCES FINAL PUBLIC REPORT

1. PROJECT INFORMATION:

Project Title:	To Improve Steam Assisted Gravity Drainage Produced Water Treatment Performance through Fundamental Understanding of Warm Lime Softening Process
Alberta Innovates Project Number:	AI2530
Submission Date:	April 15, 2020
Total Project Cost:	$96,000
Alberta Innovates Funding:	$56,000
AI Project Advisor:	Mark Donner (mark.donner@albertainnovates.ca, 780-306-2383; 780-868-8841)

2. APPLICANT INFORMATION:

Applicant (Organization):	University of Calgary
Address:	2500 University Drive, NW, Calgary, AB T2N1N4
Applicant Representative Name:	Qingye Lu
Title:	Assistant Professor
Phone Number:	(403)-210-7645; (403)-891-3986
Email:	qingye.lu@ucalgary.ca

3. PROJECT PARTNERS

We express our gratitude to our project partners for their support: Alberta Innovates Water Innovation Program, Suncor Energy, Baymag Inc., and Stantec Consulting Ltd. We thank Dr. Basil Perdicakis from Suncor Energy, Dr. David Pernitsky from Stantec Consulting Ltd., and Miss Maryam Jafari from Baymag Inc. for providing their insight and expertise from the oil sands industry that greatly assisted and facilitated the research. Also, we appreciate the advisors from Alberta Innovates especially Dr. Mark Donner and Mrs. Susan Carlisle for their guidance and suggestion on this project.

A. EXECUTIVE SUMMARY

There is a constant need to reduce operational cost and improve performance of process units in oil-sand water treatment facilities. Warm lime softening (WLS) is commonly used to reduce hardness, silica and organic matter in produced water (PW). The process relies on the use of lime ($Ca(OH)_2$), magnesium oxide (MgO), coagulant in the rapid mixing zone and flocculant in the slow mixing/settling zone. Any off-specification overflow from the WLS unit could lead to catastrophic failures in the downstream once through steam generators (OTSGs). The primary objectives of this study were:

i) to understand the electrokinetic properties and interactions of the common particles in the SAGD PW under various experimental parameters such as pH, temperature, aging, dissolved ions, and in the presence of other contaminants observed in PW;

ii) to study the impact of solution chemistry on the coagulant/flocculant demand of synthetic SAGD PW. Solution chemistry was altered by varying the concentrations of magnesium chloride ($MgCl_2$), calcium chloride ($CaCl_2$), $Ca(OH)_2$, MgO, sodium bicarbonate ($NaHCO_3$), soda ash (Na_2CO_3), clay, silica, and humic acid to simulate potential spikes in WLS feed water and varied addition of lime, soda ash and MgO during the treatment.

The zeta potential of particles is a function of surface charge which is highly sensitive to the presence of potential determining ions (PDIs) on the particle-solution interface. Data showed that the particle surface charge is determined by the acid (H^+), base (OH^-), carbonate and bicarbonate ions, divalent metal cations, and other dissolved matter such as silicate, and humic acid. These results are supported by the charge development theory, according to which, adsorption of various cationic and anionic species on the particle surface could result in dramatic change of its surface charge property.

The influence of different individual components in a representative WLS sample on the optimum dose of polymeric quarternary ammonium salt coagulant was also studied in controlled conditions. Results indicated that dissolved organic matter (represented by humic acid) and silica strongly influence the dose of the coagulant. The coagulant dose is also driven by lime and MgO present in the system – increasing the lime and MgO doses results in increasing and decreasing demand of coagulant, respectively. Dissolved salts ($MgCl_2$ and $CaCl_2$) do not significantly influence the coagulant dose. Tests with added bicarbonate and carbonate alkalinity show that coagulant dose needs to be increased with increasing alkalinity. The coagulant dose increases slowly with the increasing alkalinity (as sodium carbonate), but in case of sodium

bicarbonate the dose remains about unchanged. Bentonite clay does not have any effect on coagulant dose up to 5 ppm but coagulant dose needs to be increased after its concentration reaches 10 ppm.

The results of this study improved the understanding of fundamental properties related to particles and inter-particle interactions, together with the impact of solution chemistry on coagulation, which are highly relevant to WLS onsite chemical dosage evaluation and greater operational control. The application of this knowledge will help to minimize operational cost (less chemical addition) and improve the performance of WLS by understanding the key contributing factors for coagulant dose.

B. INTRODUCTION

Sector introduction

Steam Assisted Gravity Drainage (SAGD) operation in oil sands consumes large volumes of water. Producers in Alberta and around the world aim to enhance the efficiency of SAGD and reduce freshwater consumption through improvements to critical water treatment processes for SAGD operation. The recycling and reuse of SAGD produced water (PW) depends on its water quality. SAGD PW is typically first treated in a warm lime softening (WLS) unit to reduce hardness, silica, and organic matter content. The fundamental understanding of electrokinetic properties of particles and their interactions is essential to guide and optimize SAGD PW treatment, and has the potential significantly improve water treatment performance, reduce freshwater consumption, extend equipment service life of downstream equipment, reduce chemical expenditure, improve water recycle efficiency, reduce greenhouse gas emissions, and reduce water disposal.

Knowledge or Technology Gaps

No data is available on the electrokinetic properties of $CaCO_3$ and $Mg(OH)_2$ particles generated during WLS process of SAGD PW treatment. The water chemistry of SAGD PW (particularly silica, clay and organic matter) and its impacts the surface charge of these particles also remains poorly understood. Therefore, a systematic electrokinetic study on $CaCO_3$ and $Mg(OH)_2$ particles in a SAGD WLS is of significant value. Another related knowledge gap is that how coagulant interacts with $CaCO_3$ and $Mg(OH)_2$ particles to attain a charge neutralization for the settling of these particles in the presence of silica, clay and natural organic matter. This project resolves these critical knowledge gasps, which can provide guideline for onsite chemical evaluation and operational adjustment during WLS process upsets.

C. PROJECT DESCRIPTION

Knowledge or Technology Description

The original objectives of the project were: (1) to resolve critical knowledge gaps in WLS process; and (2) to optimize the existing WLS practice, which will lead to reduced water consumption, wastewater disposal, CO_2 emission, chemical expenditure as well as extended work life of SAGD produced water treatment facilities.

The critical knowledge gaps which need to be resolved include: (1) how $CaCO_3$ and $Mg(OH)_2$ particles generated during WLS interact with each other? (2) how a coagulant interacts with $CaCO_3$ and $Mg(OH)_2$ particles generated during WLS? (3) how the SAGD PW water chemistry including the presence and concentration of silica, suspended solids and natural organic matter affects coagulant demand during settling of the $CaCO_3$ and $Mg(OH)_2$ particles?

Updates to Project Objectives

Discussions were held on a regular basis with our industrial partners as the project progressed. The objectives of the project remained largely the same, but were updated as follows: (1) to systematically study the electrokinetic properties and interactions of $CaCO_3$ and $Mg(OH)_2$ particles in WLS at various controlled experimental conditions including pH, temperature, aging, and addition of other ions and particles such as CO_3^{2-}, HCO_3^-, Mg^{2+}, clay, humic acid (TOC), and silica; (2) to investigate how solution chemistry impacts the dosage of polyamine based coagulant and flocculant – the solution chemistry includes varying the concentration of $MgCl_2$, $CaCl_2$, $NaHCO_3$, Na_2CO_3, $Ca(OH)_2$, MgO (fresh and slaked), clay, Na_2SiO_3, and humic acid added to synthetic water samples.

Performance Metrics

The project trained 5 HQPs in total. Two graduate students, two postdoctoral research associates and one summer undergraduate student worked on this project and they have gained extensive knowledge and experience in water chemistry characterization, surface and interfacial sciences, instrumental analysis, chemistry modeling, preparation of project report and manuscript. The two graduate students will graduate this year. The two postdocs continue to work in the group. The summer student will join the group as graduate student in Sept 2020.

The project will generate two master theses, 4 journal papers and one conference paper so far. One manuscript regarding the electrokinetic properties of $CaCO_3$ and $Mg(OH)_2$ particles in lime softening has been prepared and will be submitted soon, another manuscript regarding the impact of solution chemistry on coagulant dosage in warm lime softening of SAGD produced water has been prepared and is under revision. Another two manuscripts on silica reduction mechanisms have been in preparation. One international water congress (IWC) conference paper is in preparation and will be presented at the conference in November 8-11 in San Antonio, TX.

The findings from this project may be applied to optimize warm lime softening process of SAGD produced water treatment. For example, it was found from this project that temperature affects the surface charge of $CaCO_3$ and $Mg(OH)_2$ particles, and the zeta potential of precipitated $CaCO_3$ and $Mg(OH)_2$ particles may be different for cold, warm and hot softening processes. The industrial wide bench-scale Jar testing for selecting and optimizing coagulant needs to be conducted at the same temperature as the real lime softening process, as bench-scale Jar testing conducted at room temperature will probably provide misleading results for higher temperature lime softening processes. Selecting and optimizing coagulant at the same temperature as the real lime softening process will avoid over or under dosage of coagulant, leading to optimum lime softening performance, increased SAGD produced water treatment efficiency.

D. METHODOLOGY

Chemicals

Calcium chloride dihydrate ($CaCl_2.2H_2O$, ACS reagent, 99+%), magnesium chloride hexahydrate ($MgCl_2.6H_2O$, ACS reagent, 99+%), sodium bicarbonate ($NaHCO_3$, ≥ 99.7%), sodium carbonate (Na_2CO_3, anhydrous, ≥ 99.5%) and sodium hydroxide (NaOH, ACS reagent, ≥ 97%) were purchased from Fisher Chemicals. Calcium carbonate ($CaCO_3$, Reagent Plus, ≥99%), calcium hydroxide ($Ca(OH)_2$), puriss, p.a.≥96%), magnesium hydroxide ($Mg(OH)_2$, ≥99%), sodium metasilicate (Na_2SiO_3, granular), humic acid (HA, technical), and bentonite clay ($Al_2O_3{\cdot}SiO_2{\cdot}H_2O$) were purchased from Sigma Aldrich. Milli-Q water (Millipore deionized with a resistivity of 18.2 MΩ·cm) was used for preparation of synthetic water samples.

Instruments

The ZP of the suspended particles in water samples was analyzed by a Malvern Zetasizer Nano ZS with a high concentration ZP cell (Zen1010). A Multi-Thermal Shaker (Mandel Scientific, CAN) was used for centrifuge tube mixing for section 1 experiments. pH was measured by a Fisher Scientific™ Accumet AE150 pH Benchtop Meter. A PB-900™ Series Programmable Jar Testers was used for performing jar tests (section 2 experiments). The jar tester was operated along with a temperature-controlled water bath. During the jar test, a heater and temperature switch was used to heat up the water samples and maintain the temperature at 65 °C. A VWR® general-purpose water bath with built-in temperature control was used to heat up the water samples and maintain the temperature at 65 °C after the jar test was complete. An Inkbird temperature switch was used to control water sample temperature with a temperature range of -40 to 100°C. A portable heater was used along with the Inkbird temperature switch to heat up water samples to 65°C. A UV-visible spectrometer (Shimadzu UV-2600) was used to analyze the concentration of HA in the water samples. Thermo Scientific™ iCAP™ 7200 inductively coupled plasma optical emission spectrometer (ICP-OES) was used to characterize the concentration of ions (Ca, Mg, Si) in the water samples. The magnesium oxide powder used in the silica reduction experiments was characterized by powder X-ray diffraction (PXRD) with a Rigaku Multiflex X-ray diffractometer. Image analysis of both MgO and the precipitate particles was carried out with a NanoScience Phenom ProX desktop scanning electron microscope (SEM) configured with an energy dispersive X-ray analyzer (EDS system) to perform elemental analysis of solids. Samples were tested for the surface area and porosity using the Gemini VII Series Surface Area Analyzer (Micromeritics) under liquid nitrogen. Size distribution of MgO sample was determined by a Laser Diffraction Particle Size Analyzer (LS 13-320).

Water Sample Preparation and Testing Procedure

Fresh stock solutions of $CaCl_2$, Na_2CO_3, $MgCl_2$, NaOH, and $NaHCO_3$ were prepared. $CaCl_2$ and Na_2CO_3 stock solutions were used to precipitate $CaCO_3$ in-situ; $MgCl_2$ and NaOH stock solutions were used to precipitate $Mg(OH)_2$ in-situ. Water samples containing preformed $CaCO_3$ and $Mg(OH)_2$ were also prepared. The water samples were prepared in 50 mL plastic centrifugation tubes which were placed in the Multi-Thermal Shaker mixed at 200 rpm for 5 min.

For each sample prepared, the effect of pH, temperature, aging and solution chemistry on its particle charge was studied. NaOH (1 M) and HCl (1 M) solutions were used for pH adjustment. pH was controlled between 9 – 11.5 to simulate a typical WLS processing environment. The high concentration cell used has a temperature limit of 70 °C, hence a temperature upper limit of 65 °C was applied. The temperature of water samples was manipulated at 25, 35, 45, 55, and 65°C.

To study the factors deciding coagulant dose, concentrations of Mg^{2+}, Ca^{2+}, bicarbonate, humic acid, silica, MgO, $Ca(OH)_2$, carbonate, and clay were systematically varied and the optimum coagulant dosage was measured experimentally. The water bath was used to prepare synthetic SAGD water samples at high temperature (65 °C). Then the water samples were mixed with $Ca(OH)_2$ and MgO while being stirred at 200 rpm in the jar tester. After lime softening, coagulant was added and sample was mixed for 2 min at 200 rpm to simulate rapid mixing in WLS. The coagulant doses were varied at four different concentrations of above mentioned WLS components. For the particles in each water sample, zeta potential was measured both before and after coagulant dosage and was used to optimize coagulant dosage.

Zeta Potential (ZP) Measurement

The ZP of the particle is calculated from the measured electrophoretic mobility (i.e., velocity) using the following Henry equation:

$$U_E = 2\varepsilon\zeta F(\kappa a)/3\eta \qquad (1)$$

Where U_E is the electrophoretic mobility, ε is the dielectric constant of water, ζ is the ZP, η is the water viscosity, and $F(\kappa a)$ is the Henry function. For water treatment applications, this equation is simplified by replacing $F(\kappa a)$ with the constant 1.5, which is referred to as the Smoluchowski Equation.

Prediction of Precipitates Using Thermodynamic Modeling

The potential precipitates under different conditions (pH, temperature, CO_2 exposure, chemical species, etc.) were predicted by calculating saturation indices of the possible species using thermodynamic modeling with software (Visual MINTEQ, ver. 3.1). The saturation index (SI) is defined as

$$SI = \log\frac{IAP}{K_{SP}} \qquad (2)$$

where *IAP* is the ionic activity product in the chemical reaction and K_{sp} is the solubility product of the precipitate. The *SI* indicates the potential of a specific precipitate to be formed. When $SI > 0$, the solution is supersaturated and the precipitate can form; when $SI < 0$, the solution is undersaturated and the precipitate cannot form; when $SI = 0$, the solution is in equilibrium. For a given cation, the most supersaturated solid will precipitate first.

E. PROJECT RESULTS

The project work plan and tasks are divided into specifically two major sections based on the discussions held with our industrial partners:

Section 1 - Electrokinetic study of particles in warm lime softening of steam-assisted gravity drainage (SAGD) produced water: to systematically study the electrokinetic properties and interactions of $CaCO_3$ and $Mg(OH)_2$ particles which are commonly present in WLS at various controlled experimental conditions which include pH, temperature, aging, and addition of other ions and particles such as CO_3^{2-}, HCO_3^-, Mg^{2+}, clay, humic acid (TOC), and silica.

Section 2 - Quantifying the impact of solution feed deviations on coagulant dosage in synthetic SAGD produced water: to investigate how solution chemistry affects the dosage of polyamine based coagulant and flocculant – the solution chemistry includes varying the amount of $MgCl_2$, $CaCl_2$, $NaHCO_3$, Na_2CO_3, $Ca(OH)_2$, MgO (fresh and slaked), clay, Na_2SiO_3, and humic acid added to synthetic water samples.

The following metrics have been successfully achieved. HQP were trained in water chemistry characterization, surface and interfacial sciences, instrumental analysis, chemistry modeling, preparation of project report and manuscript. The manuscripts preparation for publication in scientific journals is in progress. The results of this project are divided into two sections. Section 1 study provides the development of sound interpretation of particle charge development and knowledge specific to WLS. Section 2 study provides qualitative and quantitative analysis of factors attributing to the polyamine coagulant/flocculant dosage in WLS. The results from this project are very relevant to WLS onsite coagulant and flocculant selecting and dosage evaluation, providing practical guideline for WLS operation optimization.

1. Section 1- Electrokinetic Study of Particles in Warm Lime Softening of Steam-Assisted Gravity Drainage (SAGD) Produced Water

This section aims to understand the interactions and electrokinetics of the two most common particles in WLS, namely, calcium carbonate ($CaCO_3$) and magnesium hydroxide ($Mg(OH)_2$). Effects of various experimental parameters such as pH, temperature, aging, dissolved ions on the electrokinetic properties of $CaCO_3$ and $Mg(OH)_2$ particles were individually studied by investigating their zeta potential (ZP) values. The interactions between particles ($CaCO_3$, $Mg(OH)_2$, silicate, humic acid, clay) were also investigated. Thermodynamic modeling using Visual MINTEQ software was used to predict precipitates as a function of solution chemistry and assist with data interpretation.

Based on charge development theory, the potential species and charge development on the surface of $Mg(OH)_2$ and $CaCO_3$ in water are shown in **Figure 1.1**. The ZP, which is a function of surface charge, is directly related to the adsorption of primary dominant ions (PDIs) on the particle-solution interface. Data showed that the particle surface charge is sensitive to the acid (H^+), base (OH^-), carbonate and bicarbonate ions, divalent metal cations, and other dissolved matter such as silicate and HA. Furthermore, the ZP of preformed $CaCO_3$ and $Mg(OH)_2$ particles can vary drastically from the corresponding in-situ precipitated particles.

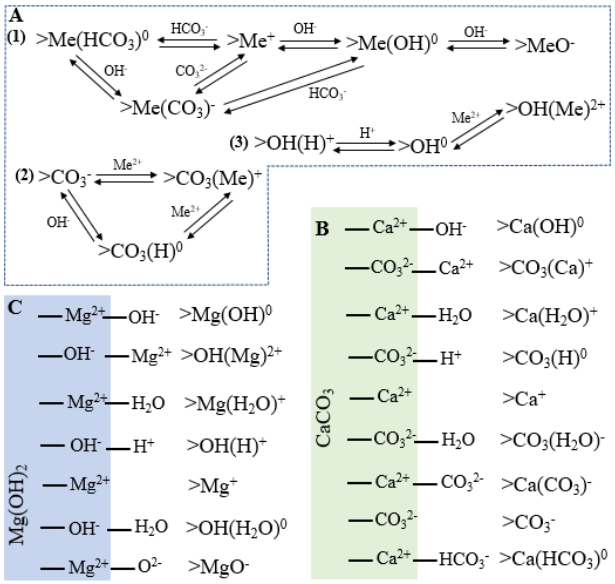

Figure 1.1. (A) Potential species and charge development on the surface of metal carbonate and metal hydroxide (Me representing metal ions), e.g., on (B) $Mg(OH)_2$ and (C) $CaCO_3$ in water.

1.1. The ZP of $Mg(OH)_2$ Particles

1.1.1. The effect of pH

The ZPs of freshly precipitated and preformed $Mg(OH)_2$ particle were measured using the aforementioned technique under various pHs at 25 °C. The pH values of both freshly precipitated and preformed $Mg(OH)_2$ were titrated to pHs of 9.0, 10, 10.5, 11.5, 12, and 12.5 from their initial conditions (pH of 10.76 and 10.30 for the freshly precipitated and preformed $Mg(OH)_2$, respectively). Both particles presented a positive charge at their initial solution pH (**Figure 1.2A**). Based on charge development theory (**Figure 1.1C**), the positive charges could be due to the $>OH(Mg)^{2+}$, $>Mg^{+}$, $>OH(H)^{+}$, $Mg(H_2O)^{+}$, and less adsorption of OH^- onto the surface. Increasing pH after the initial point led to a reduction in the ZP, which is also aligned with the charge development theory, as at higher pH one would expect $>MgO^-$ to increase (**Figure 1.1C)**. At the same pH, the ZP of the freshly precipitated was higher than that of preformed $Mg(OH)_2$.

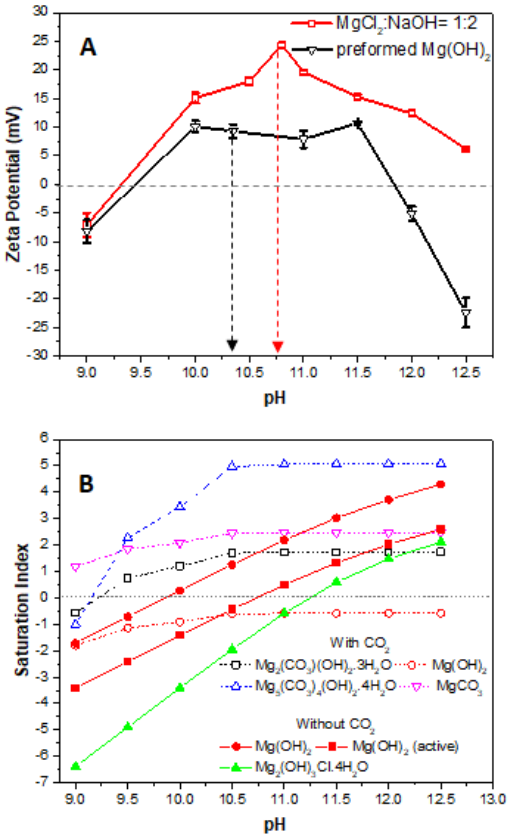

Figure 1.2. (A) The effect of pH on the ZP of freshly precipitated and preformed $Mg(OH)_2$ in water at 25 °C (dashed arrows indicating initial pH of the water samples). (B) The saturation indices (SIs) of magnesium minerals at different pH for freshly precipitation case with and without CO_2 impact (the partial pressure of CO_2 PCO_2 = 0.00038 atm).

Reducing the initial pH to 10 did not affect the ZP of preformed $Mg(OH)_2$ but lowered that of freshly precipitated from ~25 to ~20 mV (**Figure 1.2A**). At a pH of 9, negative ZP was recorded. This could not be explained by changes in H^+ or OH^- ions. Chemistry modeling without CO_2 effect also indicated that $Mg(OH)_2$ is undersaturated when pH is lower than 10 or 10.5 depending on the crystal structure (**Figure 1.2B**). The negative charge at pH of 9 is likely due to the dominating presence of magnesite ($MgCO_3$) when the sample was exposed to air. Saturation indices (SIs) predicted from chemistry modeling as a function of pH at 25 ^oC and atmospheric pressure indicated the precipitation of $MgCO_3$ at pH of 9. The chemistry modeling also suggested that hydromagnesite [$Mg_5(CO_3)_4(OH)_2{\cdot}4H_2O$] and artinite [$Mg_2(OH)_2CO_3{\cdot}3H_2O$] precipitate at pH > 9.5. At a pH of 9, the only predicted precipitate was $MgCO_3$ when the sample reached equilibrium with atmospheric CO_2. The lower ZP of preformed $Mg(OH)_2$ than that of freshly precipitated $Mg(OH)_2$ is likely due to some carbonate species existed on the surface of preformed one at the initial point.

1.1.2. The effect of temperature

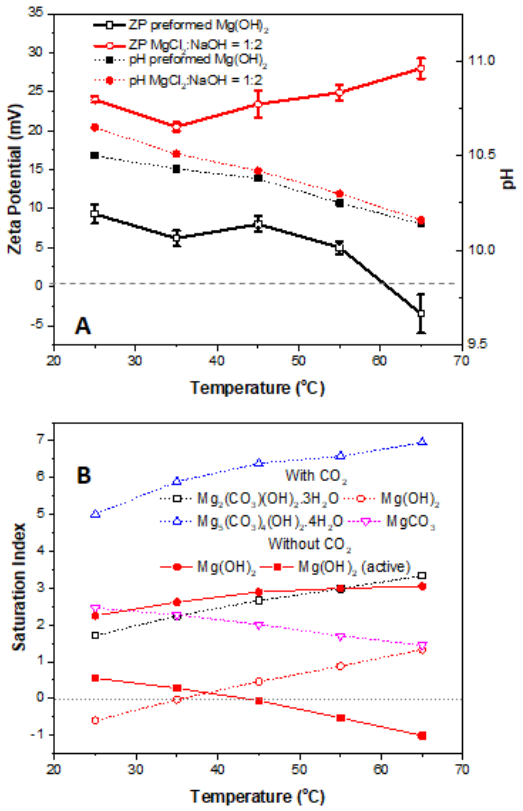

Figure 1.3. The effect of temperature on the (A) pH and ZP of freshly precipitated and preformed $Mg(OH)_2$ in water. (B) The SIs of magnesium minerals for freshly precipitation case WS 1.1 as a function of temperature with and without CO_2 impact (P_{CO2} = 0.00038 atm).

The previously examined water samples of freshly precipitated and pre-formed $Mg(OH)_2$ particles were further examined at temperatures up to 65 °C. The measured pHs and ZPs as a function of temperature are shown in **Figure 1.3A**. While the resulting pH of both freshly precipitated and preformed $Mg(OH)_2$ particles decreased with increasing temperature, the ZPs of the freshly precipitated and preformed $Mg(OH)_2$ particles followed opposite trends. **Figure 1.3A** shows that the ZP of freshly precipitated $Mg(OH)_2$ increased slowly from ~ 22 mV (25 °C) to ~ 27 mV (65 °C). $Mg(OH)_2$ solubility decreases with increasing temperature. This indicates the pH would decrease which aligned with our observation. So the possible explanation for increase in the ZP of the freshly precipitated $Mg(OH)_2$ particles is the shifting of $>Mg(OH)^0$ to $>Mg^+$ due to the decreased pH (**Figure 1.1A**).

In the case of preformed $Mg(OH)_2$ particles, the ZP was positive between 25 to 45 °C but much lower compared to the freshly precipitated one (~ 5 mV vs ~ 20 mV at 25 °C). Furthermore, the minor change in ZP indicates that the temperature range tested has very little impact on the interaction between the particles and the surrounding medium. However, the ZP decreased when the temperature was raised to 55 °C and became negative at 65 °C (~ -5 mV). The reversal of charge from positive to negative cannot be

explained by the above-mentioned equilibrium (**Figure 1.1**). It is also an indication of possible incorporation of new mineral species on the surface with inherent negative charge.

Chemistry modeling predicted the solid phase that could be formed at different temperature based on the species present in the solution for freshly precipitation and preformed $Mg(OH)_2$ in **Figure 1.3B**. For the freshly precipitation case, the calculated SIs (with CO_2) indicate that artinite ($Mg_2(OH)_2CO_3{\cdot}3H_2O$), hydromagnesite ($Mg_5(CO_3)_4(OH)_2{\cdot}4H_2O$), and magnesite ($MgCO_3$) are the insoluble minerals below 35 °C; while above 35 °C, brucite also precipitates. Additionally, with increasing temperature, the SI of $MgCO_3$ decreases and that of $Mg_2(OH)_2CO_3{\cdot}3H_2O$, $Mg_5(CO_3)_4(OH)_2{\cdot}4H_2O$ and brucite increases. $Mg_2(OH)_2CO_3{\cdot}3H_2O$ always has the highest SIs (with CO_2) for freshly precipitation case (**Figure 1.3B**). For the preformed $Mg(OH)_2$, brucite is at equilibrium throughout and $Mg_5(CO_3)_4(OH)_2{\cdot}4H_2O$ has higher SIs (without CO_2) at high temperature (65 °C). It is likely higher concentration of CO_3^{2-} on the surface of preformed $Mg(OH)_2$ at 65 °C account for the negative ZP measured.

1.1.3. The effect of aging

Aging of sample is a critical factor in WLS since prolonged sample holding time leads to increase in the concentration of dissolved CO_2 in solution. As the CO_2 concentration increases, the pH and total alkalinity change with time which could result in changing of charge on the particle surface. The freshly precipitated and preformed $Mg(OH)_2$ in water were left exposed to the ambient CO_2 for 48 h. The pH and ZPs of both particles were measured at different time intervals.

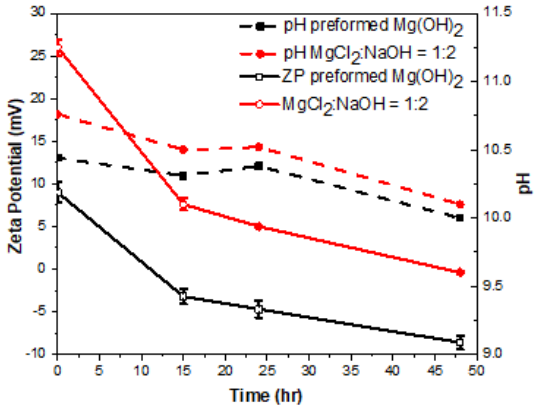

Figure 1.4. (A) The pH and ZP of freshly precipitated and performed Mg(OH)2 in water during aging 25 °C.

As shown in **Figure 1.4**, the pH of both water samples decreased with exposure time to the ambient CO_2, a phenomenon commonly observed in aqueous solution due to the increase of carbonic acid as CO_2 dissolves. The ZPs of both particles also follow a decreasing trend with time – for the freshly precipitated $Mg(OH)_2$, ZP was reversed to negative. This could be due to the increase of PDIs such as HCO_3^- and CO_3^{2-} in the solution when the water sample was exposed to the atmospheric conditions. The SIs predicted from thermodynamic modeling indicated that with aging, $Mg_2(OH)_2CO_3{\cdot}3H_2O$, $Mg_5(CO_3)_4(OH)_2{\cdot}4H_2O$ and $MgCO_3$ can precipitate. This is a reasonable prediction and formation of OH^- and CO_3^{2-} rich species can account

for the negative ZP with time. As discussed below, adding HCO_3^- and CO_3^{2-} ions into the solution of $Mg(OH)_2$ indeed decreased the ZP and even reversed the ZP to negative, thus confirming our argument.

1.4. The effect of $NaHCO_3$ and Na_2CO_3

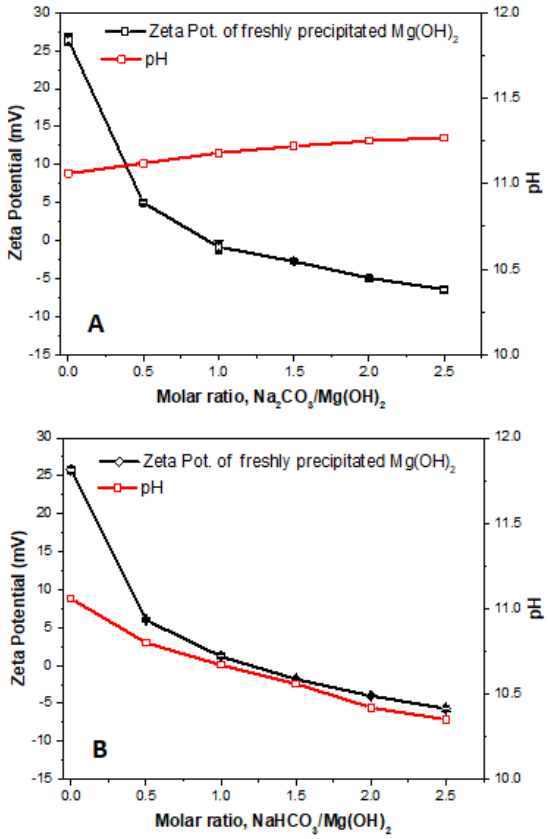

Figure 1.5. The effect of (A) Na_2CO_3 and (B) $NaHCO_3$ on the pH and ZP of $Mg(OH)_2$ 25 ^oC.

The effect of $NaHCO_3$ and Na_2CO_3 addition on $Mg(OH)_2$ (freshly precipitated) was studied (**Figure 1.5**). As $NaHCO_3$ solution was added, a steady decrease in the pH from ~11 to 10.3 was observed. This was accompanied by a rapid decrease in the ZP initially from 25 mV to ~ 5 mV and a slow decrease until the ZP became negative. In the case of Na_2CO_3 addition, a similar trend was observed in the ZP, although the pH showed an increase from 11 to 11.25. Based on thermodynamic modeling, the predicted species with SIs greater than zero are $Mg_5(CO_3)_4(OH)_2{\cdot}4H_2O$, $MgCO_3$, and $Mg_2(OH)_2CO_3{\cdot}3H_2O$, respectively in descending order. As discussed in the temperature effect section, the formation of OH^- and CO_3^{2-} rich species can account for the negative ZP after the addition of $NaHCO_3$ and Na_2CO_3.

1.2. The ZP of $CaCO_3$ Particles

1.2.1. The effect of pH

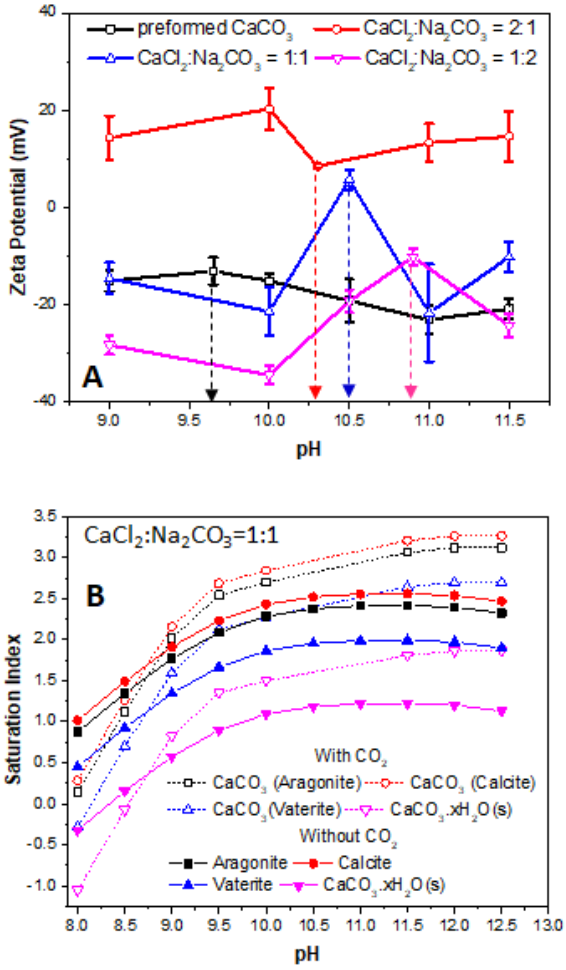

Figure 1.6. (A) The effect of pH on the ZP of $CaCO_3$ 25 °C (dashed arrows indicating initial pHs of the water samples). (B) The SIs of mineral species as a function of pH for in situ formed $CaCO_3$ case with and without CO_2 impact ($CaCl_2$:Na_2CO_3 = 1:1, P_{CO2} = 0.00038 atm). Modeling for other $CaCl_2$:Na_2CO_3 ratios, and preformed $CaCO_3$ case are shown in Figure S5 and S6, respectively.

The ZPs of preformed $CaCO_3$ and freshly precipitated $CaCO_3$ were measured at 25 °C, from pH 9 to 11.5 (**Figure 1.6A**). The three different samples of freshly precipitated $CaCO_3$ were prepared by varying molar ratios of $CaCl_2$ to Na_2CO_3 from 2:1 to 1:1 to 1:2, respectively. The ZP of the performed $CaCO_3$ was negative throughout the pH range tested (9 – 11.5) which is consistent with other reported studies.

The freshly precipitated $CaCO_3$ with molar ratios of $CaCl_2$:Na_2CO_3 of 2:1 and 1:1 showed positive ZP, while the freshly precipitated $CaCO_3$ with molar ratio of 1:2 showed negative ZP (**Figure 1.6A**). For freshly precipitated $CaCO_3$ ($CaCl_2$:Na_2CO_3 = 2:1), its ZP was positive throughout the pH range tested. The positive

ZP can be attributed to the presence of excess Ca^{2+} ions and one would expect the $>CO_3H^0$ functional group shifts to $>CO_3Ca^+$ which could lead to positively charged $CaCO_3$ particles. The increasing pH could diminish the positive charge. Similar effect was observed in presence of Mg^{2+} ions which was discussed later. This is further supported by the fact that reducing the molar ratio of $CaCl_2$ to Na_2CO_3 also lowered the ZP. For freshly precipitated $CaCO_3$ ($CaCl_2$:Na_2CO_3 = 1:1), its ZP at initial pH was slightly positive but dropped to negative at other tested pHs. The drop of ZP at higher pHs could be due to the adsorption of OH^- onto the CaCO3 particle surface shifting functional groups to $>CaO^-$ and $>CO_3^-$. ZP was also observed to decrease after the initial point when pH was lowered. At lower pHs, one would expect dissolution of precipitated $CaCO_3$ which results in both increase of Ca^{2+}, CO_3^{2-} and HCO_3^- ions. It is likely that CO_3^{2-} and HCO_3^- ions were favored to be adsorbed onto the $CaCO_3$ particles, which would exhibit less $>Ca^+$, more $>Ca(HCO_3)^0$ and $>Ca(CO_3)^-$ functional groups based on the functional group theory (**Figure 1.1**). The slight bounce in ZP at pH of 9 could be led by the adsorption of free Ca^{2+} ions onto the $CaCO_3$ particles which could exhibit some $>CO_3Ca^+$ functional groups. For freshly precipitated $CaCO_3$ ($CaCl_2$:Na_2CO_3 = 1:2), its ZP was negative throughout the pH range tested, which is accounted for by the excess of carbonate ions in the solution. The trend of ZP change was very similar to that of freshly precipitated $CaCO_3$ ($CaCl_2$:Na_2CO_3 = 1:1). The ZP was initially negative. When pH increased after the initial point, the ZP dropped which is aligned well with the functional group theory due to more $>CaO^-$and $>CO_3^-$ functional groups on the surface. With decreasing pH from the initial point, more $>Ca(CO_3)^-$ functional groups were expected on $CaCO_3$ particles due to the presence of CO_3^{2-} and HCO_3^- ions. The slight bounce in ZP at pH of 9 could be led by the adsorption of free Ca^{2+} ions onto the $CaCO_3$ particles which could exhibit some $>CO_3Ca^+$ functional groups.

Simulation of the solution chemistry in different conditions (**Figure 1.6B**) showed that the mineral species with SIs greater than zero for in situ formed $CaCO_3$ cases were calcite > aragonite > vaterite > $CaCO_3{\cdot}xH_2O$ in a descending order, with a slightly higher SIs with CO_2 input than that of without. The SIs predicted for calcite (preformed $CaCO_3$) was zero for the entire pH range, implying an equilibrium between dissolved and precipitated $CaCO_3$.

1.2.2. The effect of temperature

The zeta potentials (ZPs) of preformed $CaCO_3$ and freshly precipitated $CaCO_3$ were measured under various temperatures (**Figure 1.7**). The pH of the preformed $CaCO_3$ remained fairly stable, whereas the ZP decreased from -12 mV to -22 mV.

For freshly precipitated $CaCO_3$, temperature change showed effects depending on the initial molar ratios of precursor materials ($CaCl_2$:Na_2CO_3). Both $CaCl_2$:Na_2CO_3 = 1:1 and $CaCl_2$:Na_2CO_3 = 2:1 showed similar trends of pH and ZP. For $CaCl_2$:Na_2CO_3 = 1:1, the pH of the particles started around 10 and decreased with increasing temperature (9.5 at 65 ^oC). The ZP became more positive (5 to 15 mV) as the temperature increases. For $CaCl_2$:Na_2CO_3 = 2:1 (excess Ca^{2+} ions), the pH was 9.7 and decreased with increasing temperature (8.3 at 65 ^oC). The ZP was around 20 mV initially and increased further with increasing temperature. For the case of $CaCl_2$:Na_2CO_3 = 1:2 where the water sample has excessive CO_3^{2-} ions, the pH remained very close to 11 and the ZP became more negative as the temperature increased following the trend of preformed $CaCO_3$.

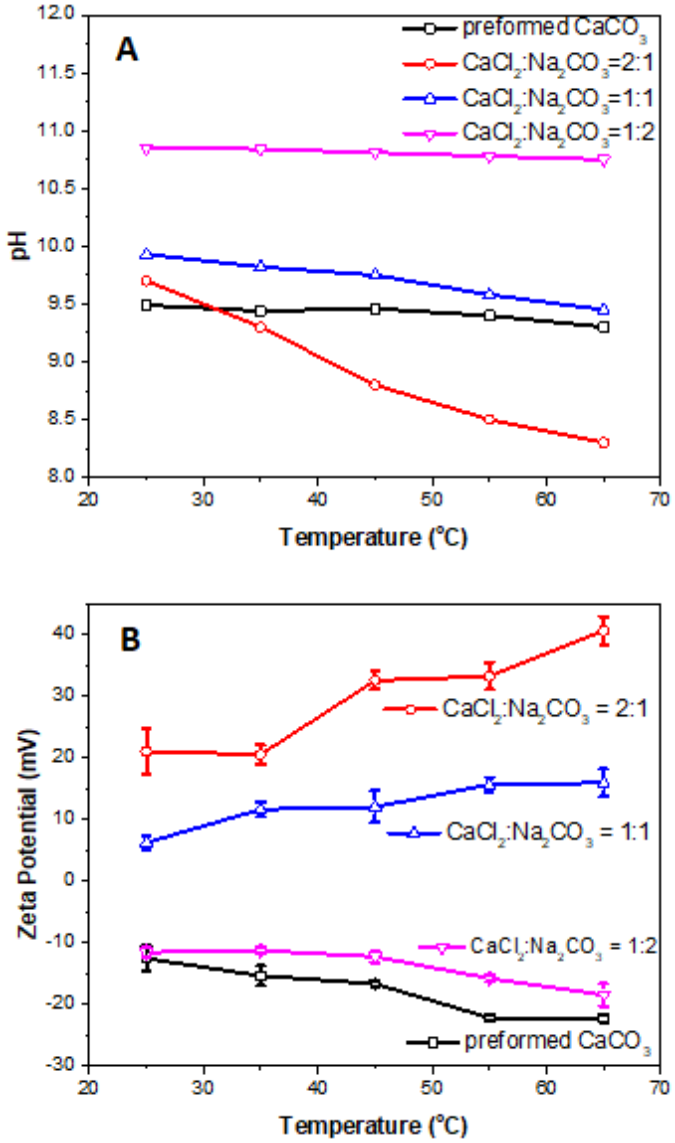

Figure 1.7. The effect of temperature on the (A) pH, and (B) ZP of $CaCO_3$.

The predicted mineral species in descending order of SI for in situ formed samples with CO_2 input were calcite, aragonite, vaterite, and $CaCO_3.xH_2O$, respectively. Interestingly, no significant change of SIs was observed with increasing temperature. The SIs of calcite slightly decrease with increasing temperature, leading to slightly reduced concentration of Ca^{2+} and CO_3^{2-}. Based on the charge development theory (**Figure 1.1**), for $CaCl_2$:Na_2CO_3 of 1:1 and 2:1, the dominant surface functions $>CO_3(Ca)^+$ and $>Ca^+$ contribute to the positive ZP at 25 °C. When temperature increases, the decreased calcite solubility probably lead to more dominant surface functions of $>CO_3(Ca)^+$ and $>Ca^+$ and corresponding more positive ZP. For $CaCl_2$:Na_2CO_3 of 1:2 and preformed $CaCO_3$, the dominant surface functional groups $>CO_3^-$ and $>Ca(CO_3)^-$ contribute to the negative ZP at 25 °C. When temperature increases, the decreased calcite solubility probably lead to more dominant surface functions of $>CO_3^-$ and $>Ca(CO_3)^-$ and corresponding more negative ZP.

1.2.3 The effect of aging

To study the effect of aging, freshly precipitated $CaCO_3$ and preformed $CaCO_3$ were exposed to the atmospheric condition for 48 h, and their ZPs and pHs were measured periodically. The observed trend in pH and ZP is shown in **Figure 1.8 A and B**, respectively. During the aging test, the pH of all water samples decreased over time due to the increased amount of dissolved CO_2. The ZP of all particles decreased over time, for freshly precipitaed $CaCO_3$ particles ($CaCl_2$:Na_2CO_3 = 2:1 or 1:1), their ZPs started being postive and were eventually reversed to negative. This result is in agreement with the adsorption of HCO_3^- on the hydrated $CaCO_3$ particles as proposed in the surface complexation model. At the end of the aging experiment, pH of all water samples ranged from 8 – 10 within which HCO_3^- is the dominating alkalintiy species. The presence of HCO_3^- would shift $>CaOH^0$ to negatively charged $>CaCO_3^-$ functional groups.

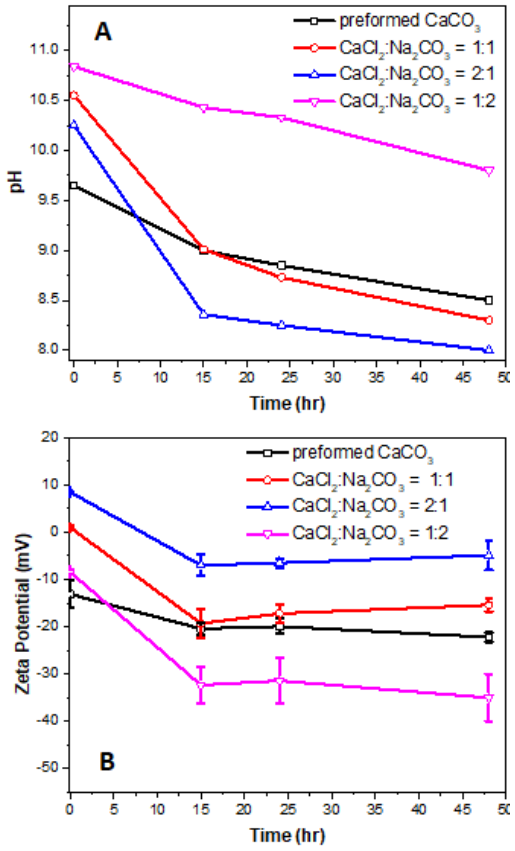

Figure 1.8. Change of (A) pH of water samples, and (B) ZP of $CaCO_3$ particles during aging 25 ^oC.

1.2.4. The effect of $MgCl_2$

$MgCl_2$ stock solution was gradually added to assess the impact of Mg^{2+} ion on the charge of preformed $CaCO_3$ particles at 25 °C. The Mg^{2+} ions had same effect on the ZP as excess Ca^{2+} ions, as discussed in the sections above. The ZP of the $CaCO_3$ was negative but was eventually reversed to positive with the addition of $MgCl_2$ (**Figure 1.9**). Upon addition of 0.5 mL of $MgCl_2$ (molar ratio of $MgCl_2$ to $CaCO_3$ ~0.5), average ZP was close to zero and addition of 2 mL of $MgCl_2$ (molar ratio of $MgCl_2$ to $CaCO_3$ >2) reversed the ZP of

$CaCO_3$ particles (588 mg/L) to positive. A study done by Black & Christman showed similar result – the mobility of $CaCO_3$ (2 mM) became zero when 80 ppm of $MgCl_2$ was added. These data concur with the proposed surface speciation of $CaCO_3$ particles $>CO_3^-$ with metal cations (Mg^{2+}) to form $>CO_3(Mg)^+$ (**Figure 1.1**). The modeling indicates the potential formation of dolomite $CaMg(CO_3)_2$.

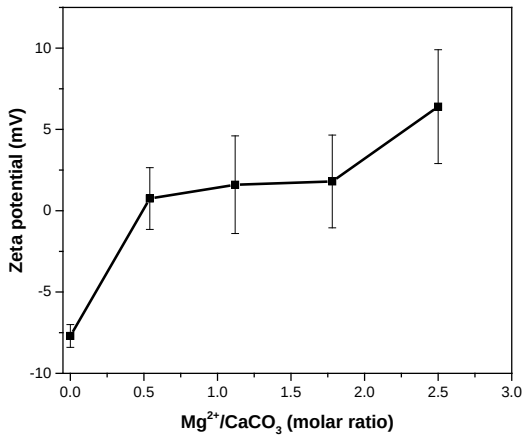

Figure 1.9. The effect of Mg^{2+} on the ZP of preformed $CaCO_3$ 25 °C

1.3. Interactions of Binary Particles

1.3.1. $Mg(OH)_2$ and $CaCO_3$ Particles

The molar ratio of $Mg(OH)_2$ and $CaCO_3$ was varied from 0 to 2 and the ZPs were measured at different temperatures (**Figure 1.10**). The ZP of the binary sysetem was negative and became positive when the molar ratio of $Mg(OH)_2$ to $CaCO_3$ was increased to 0.5. Further increasing the ratio to 1 and 2 led to a slow but steady increase in ZP at 25 °C and 45 °C. The trend was slightly different at 65 °C, where the ZP increased rapidly from molar ratio 0 to 1 and then became stable after that. Since $Mg(OH)_2$ carries positive charge and $CaCO_3$ carries negative charge, the observed change in ZP from negative to positive with increasing ratio of $Mg(OH)_2$ is reasonable. Interaction between the two particles could also lead to formation of new minerals with various compositions. The possible species in decreasing order of SIs are huntite ($CaMg_3(CO_3)_4$) > hydromagnesite ($Mg_5(OH)_2(CO_3)_4{\cdot}4H_2O$) > dolomite ($CaMg(CO_3)_2$) > magnesite ($MgCO_3$) > and artinite ($Mg_2(OH)_2CO_3{\cdot}3H_2O$).

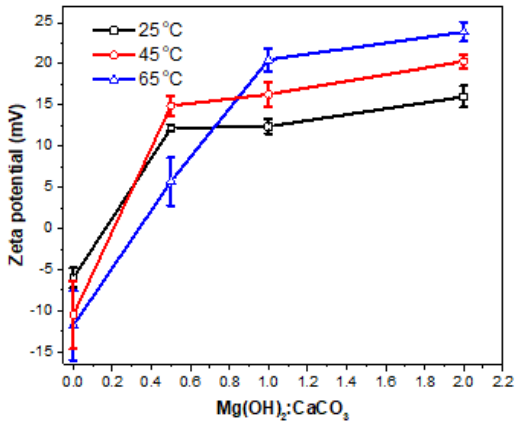

Figure 1.10. The ZP as a function of molar ratio of $Mg(OH)_2$ to $CaCO_3$.

1.3.2. The effect of silicate on the ZP of $CaCO_3$ and $Mg(OH)_2$ particles

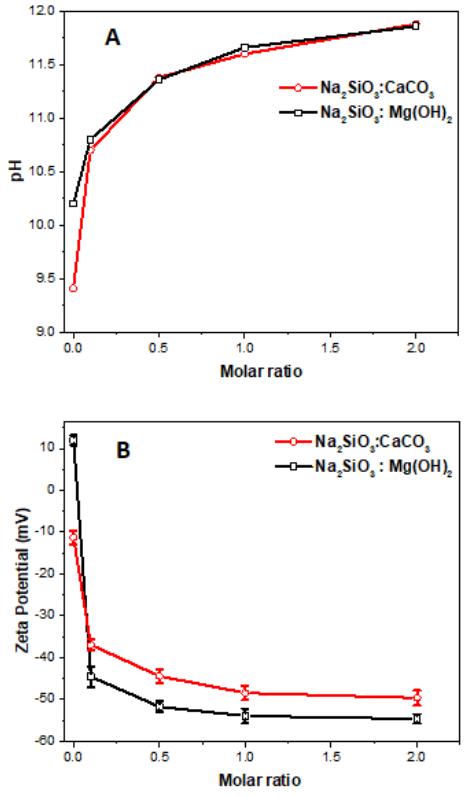

Figure 1.11. Effect of sodium silicate on the (A) pH, and (B) ZP of $CaCO_3$ and $Mg(OH)_2$ particles at 25 °C.

Silicate and organic carbon are the ubiquitous constituents of SAGD PW. The pH and ZP of $CaCO_3$ and $Mg(OH)_2$ in the presence of various amounts of Na_2SiO_3 (to represent SiO_2) and HA (to represent organic carbon) were measured. The PZC of silicate is around pH 2 – 3 implying that silicate would be negatively charged throughout the pH range tested in our study. **Figure 1.11 A** and **B** show the pH and ZPs,

respectively, as a function of molar ratios of Na_2SiO_3 and $CaCO_3$ or $Mg(OH)_2$. There was a sharp increase in pH at the molar ratio of 0.1 and then increased slowly at ratios 0.5 and higher. In the case of $CaCO_3$, ZPs showed a sharp decrease from -10 to -37 mV at molar ratio 0.1 and followed by a slow decrease to -45 mV between molar ratios 0.5 to 2. $Mg(OH)_2$ and Na_2SiO_3 system also followed the same trend with increasing ratio of Na_2SiO_3, although the final ZP was -55 mV. The negative ZP is expected to be dominated by the presence of the charged surface species of $>Si\text{-}O^-$ and a direct result of the increase in pH that shifts >Si-OH to $>Si\text{-}O^-$ from functional groups. The thermodynamic modeling indicates that there are no calcium silicate mineral formed for silicate/$CaCO_3$ system, while magnesium silicate such as chrysotile $Mg_3(Si_2O_5)(OH)_4$ may form for silicate/$Mg(OH)_2$ system.

1.3.3. The effect of humic acid (HA) on the ZP of $CaCO_3$ and $Mg(OH)_2$ particles

Similar to the silica experiments, the pH and ZP of $CaCO_3$ and $Mg(OH)_2$ in the presence of various amounts of HA were measured (**Figure 1.12**). PW organics have many humic like organic matters, most importantly in the presence of large number of negatively charged functional groups. Hence humic acid is used in this study to mimic organic matter in PW. HA reduced the pH of $CaCO_3$ and $Mg(OH)_2$ solution. With increasing concentration of HA, the pH of $CaCO_3$ solution decreased from 9.45 to 8.3 and the pH of $Mg(OH)_2$ solution decreased from 10.45 to 8.3. The ZP decreased with increasing molar ratios for both $CaCO_3$ and $Mg(OH)_2$ solutions.

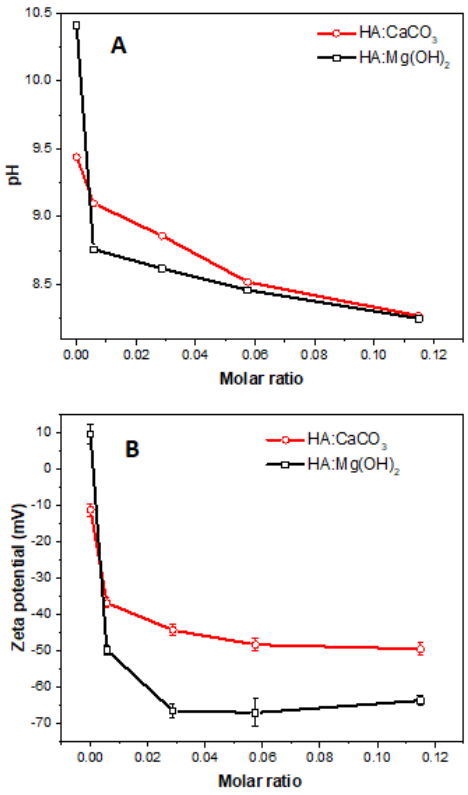

Figure 1.12. Effect of humic acid (HA) on the (A) pH, and (B) ZP of $CaCO_3$ and $Mg(OH)_2$ particles 25 °C.

The binding of metal ions to the carboxyl and hydroxyl groups on HA can occur in a monodentate and bidentate form. The Stockhom humic model (SHM) predicts that the dissolution of $CaCO_3$ and $Mg(OH)_2$ increases with the concentration of HA. Based on modeling data, the dissolved Ca^{2+} ions can form mono- and bidentate complexes, i.e., $HACa^{+}$(aq) and HA_2Ca and Mg^{2+} ions form monodentate complex, $HAMg^{+}$(aq).

1.3.4. The effect of clay on the ZP of $CaCO_3$ and $Mg(OH)_2$ particles

In some SAGD operations, tailing water, which has thousands ppm of silica, may be recycled and fed into a WLS unit along with PW. Although this stream is typically minor, it could increase clay content up to 25 ppm. Bentonite purchased from Sigma Aldrich was used to represent clay content in PW. The effect of increasing clay content on the zeta potential of the clay/$CaCO_3$ and clay/$Mg(OH)_2$ systems was studied. For both experiments, there was no obvious change of pH with the increasing clay concentration. It was observed that when introducing clay to $CaCO_3$ particles, the zeta potential of the system became more negative as more clay was added. At clay:$CaCO_3$ molar ratio of 0.05, the zeta potential was around -28 mV. Similar results were observed for the clay and $Mg(OH)_2$ interaction. Although the zeta potential of $Mg(OH)_2$ started around +10 mV, at the clay: $Mg(OH)_2$ molar ratio of 0.05, the zeta potential was around -37 mV.

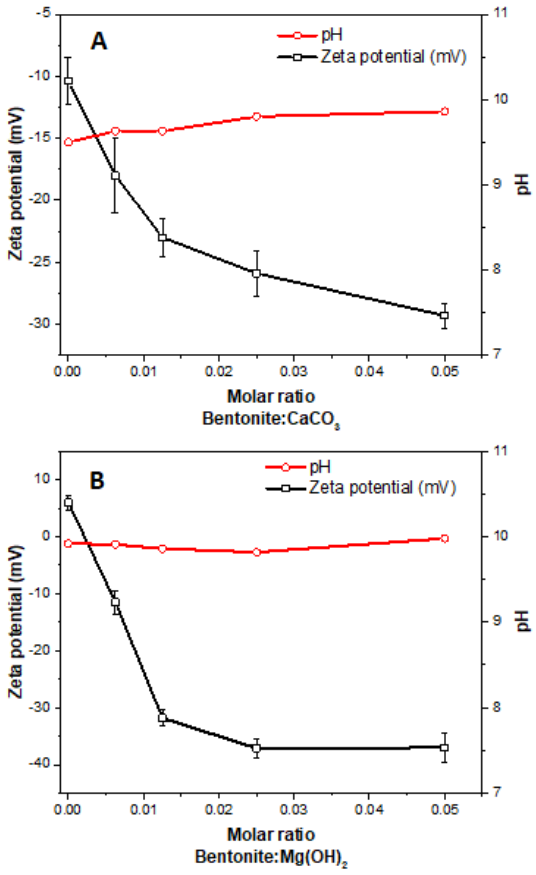

Figure 1.13. ZP of $CaCO_3$ and $Mg(OH)_2$ particles.

2. Section 2-Quantifying the Impact of Solution Feed Deviations on Coagulant Dosage in Synthetic SAGD Produced Water

A quantitative understanding of the impact of solution feed deviations on the WLS performance is critical for guiding both industrial onsite operation and technology optimization. In this section, a systematic study on the impact of solution chemistry on polyamine coagulant/flocculant demand of synthetic SAGD PW is reported. Solution chemistry was altered by varying the concentrations of magnesium chloride ($MgCl_2$), calcium chloride ($CaCl_2$), sodium bicarbonate ($NaHCO_3$), clay, silica, and humic acid to simulate potential contaminant spikes. The impact of the concentrations of added soda ash (Na_2CO_3), $Ca(OH)_2$ and MgO were also studied. Zeta potential measurements were used to determine the optimum coagulant dosage for each experiment.

Results indicate that dissolved organic matter (represented by HA) and silica strongly influence the dose of the coagulant. The coagulant dose is also driven by lime and MgO present in the system with lime increasing the coagulant dose and MgO reducing the coagulant dose. Dissolved salts, i.e. $MgCl_2$ and $CaCl_2$ do not significantly influence the coagulant dose. Tests with added bicarbonate and carbonate alkalinity show that coagulant dose is increased due to alkalinity. In case of added alkalinity, the coagulant dose increases slowly with the concentration of sodium carbonate but in case of sodium bicarbonate the dose is almost the same. Bentonite clay does not have any effect on coagulant dose up to 5 ppm but increases after 10 ppm. These results will provide practical guideline for evaluating onsite coagulant and flocculant doses in the WLS unit. Combining with the study in Section 1, understanding of the potential underlying interaction mechanisms may provide insights on future technology optimization.

2.1. Coagulant dosage as a function of the concentration of HA

As one of the natural organic matters commonly found in surface, ground, and waste waters, HA was chosen as a model organic compound and its impact on coagulant dosage was studied. **Figure 2.1A** shows the change of the zeta potential of water samples with HA concentrations range from 0 to 300 ppm with the other constituents the same as that of Benchmark water sample. Lime and MgO were added before the addition of coagulant. The initial zeta potential for all samples before the addition of coagulant was around -30 mV. With the addition of coagulant, negative charge was neutralized and the zeta potential of all samples gradually became less negative. Once the optimum dose of coagulant was added, the zeta potential was between -5 to +5 mV, indicating that the particles became almost neutral.

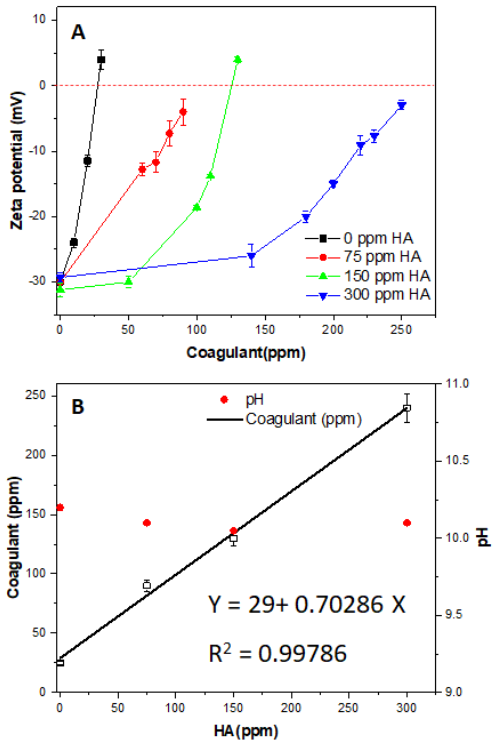

Figure 2.1. (A) the zeta potential of water samples with various HA concentrations as a function of coagulant dosage at 65 ^{o}C, and (B) corresponding optimum coagulant dosage as a function of the concentration of HA determined from the zeta potential measurements.

Figure 2.1B summarizes the coagulant dose required at various concentrations of HA added in the solution. Clearly, the coagulant dose increased with the concentration of HA in the solution. There was almost linear dependence of coagulant dosage on HA concentration (R^2 = 0.998). The slope also indicated that HA has great influence on coagulant demand. The pH of the water samples at different concentrations of HA was also measured before the addition of coagulant, which ranged between 10 and 10.2 for all the concentrations of HA, as shown in **Figure 2.1B**.

In Section 1, we have examined the pH and zeta potential of HA-$CaCO_3$ and HA-$Mg(OH)_2$ mixtures at different molar ratios. Because $CaCO_3$ and $Mg(OH)_2$ surfaces are sensitive to the changes in the medium, addition of HA in small quantities (molar ratio 0.01 to 0.1) can influence the zeta potential of the system. HA can alter the properties of $CaCO_3$ and $Mg(OH)_2$ in various possible ways: i) increased dissolution, ii) dissolved Ca and Mg form monodentate and bidentate complexes with HA and iii) high negative charge density of HA easily dominates the net charge of the colloidal suspension.

2.2. Coagulant dosage as a function of the concentration of silica

To study the impact of silica concentration on coagulant demand, solutions were prepared with 0 to 300 ppm silica, while all the other constitutents were the same as that of Benchmark water sample. As shown in **Figure 2.2A**, the zeta potential of all samples before coagulant dosage ranged from -30 to -35 mV and coagulant was added stepwise until the zeta potential increased to a value ranging between -5 to +5 mV. In the experimental conditions, silica particles are expected to present negative charges.

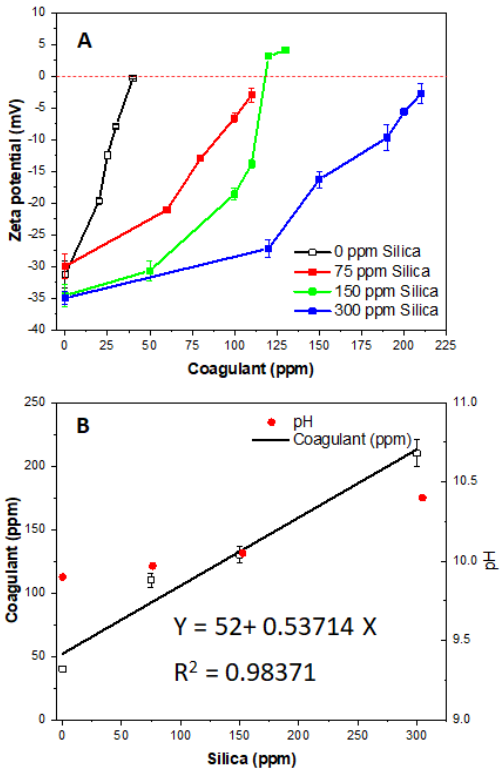

Figure 2.2. (A) the zeta potential of water samples with various concentrations of silica as a function of coagulant dosage at 65 ^{o}C, and (B) corresponding optimum coagulant dosage as a function of the concentration of silica determined from the zeta potential measurements.

As in case of HA, here also an almost linear relationship was observed between the coagulant dose and silica concentration (**Figure 2.2B**). The measured coagulant concentration was fitted to a linear equation (R2 = 0.984) although the slope was smaller (0.54 vs. 0.70) which indicates that HA has a greater influence on the coagulant dose than silica, which is indicative of higher charge density of HA than silica under the experimental conditions specified. **Figure 2.2B** also shows that in absence of silica, the pH increased with the increasing concentration of silica. Sodium metasilicate was used in this study to represent soluble silica which is responsible for increasing pH with concentration.

In Section 1, we reported the effect of silica on $CaCO_3$ and $Mg(OH)_2$ particles during WLS. The zeta potential of silica/$CaCO_3$ and silica/$Mg(OH)_2$ mixtures (molar ratio between 0.1 to 2) was negative and thermodynamic modeling suggested that added silica mainly precipitates as silica in $CaCO_3$ solution but will react with $Mg(OH)_2$ to form magnesium silicate compound.

2.3. Coagulant dosage as a function of $MgCl_2$

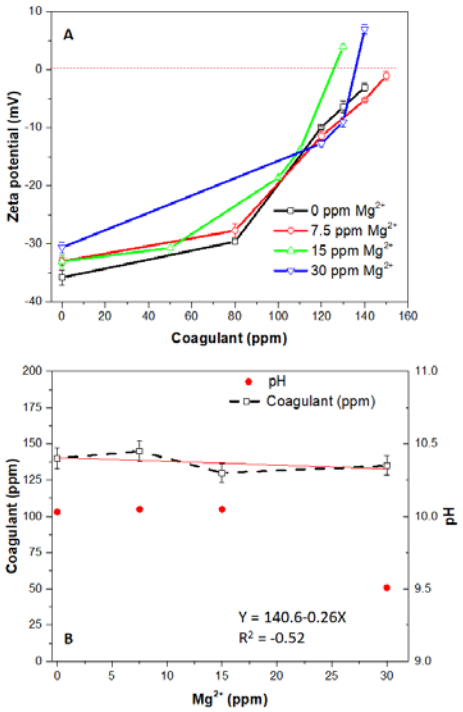

Figure 2.3. (A) the zeta potential of water samples with various concentrations of Mg^{2+} as a function of coagulant dosage at 65 ^{o}C, and (B) corresponding optimum coagulant dosage as a function of the concentration of Mg^{2+} determined from the zeta potential measurements.

Magnesium and calcium metal ions are categorized as dissovled hardness in WLS system. The influence of each of the metal ions was systematically studied. First, the impact of $MgCl_2$ on the coagulant dose was studied by changing the concenration of Mg^{2+} from 0 to 30 ppm while all the other constitutents were the same as that of Benchmark water sample. As shown in **Figure 2.3A**, the zeta potential was approximately -35 mV when no $MgCl_2$ was added and slowly became less negative with the increasing $MgCl_2$ concentration. At 30 ppm Mg^{2+} concentration, the zeta potential was -30 mV. This trend is reasonable given that the divalent metal ions can neutralize the negatiely charge groups on the suspended particles. For the given cocentration range, the coagulant dose was not strongly influenced by the concentration of dissolved Mg ions, which suggests that the total negative charge of the system is in huge excess when compared to the $MgCl_2$ added. **Figure 2.3B** shows that at 0 and 7.5 ppm, the dose was marginally greater than at 15 and 30 ppm. Based on t-test analysis, there was no significant difference between the measured dose as a function of $MgCl_2$ [t = 2.82, df = 2, p = 0.05, $t_{critical}$ = 2.92]. The pH of the system remains close to 10 at 0, 7.5 and 15 ppm Mg^{2+} but dropped to 9.5 at 30 ppm, which is due to the acidic nature of $MgCl_2$.

The effect of dissolved metal cations such as Mg^{2+} on particle charge has been reported earlier. We found that with the increasing concentration of Mg^{2+} ions, the negative charge of $CaCO_3$ suspension becomes less negative and eventually becomes positive once the concentration exceeds the overall negative charge

of the $CaCO_3$ particles. The proposed rationale is that metal cations can adsorb on the particle surface responsible for the negative charge.

2.4. Coagulant dosage as a function of $CaCl_2$

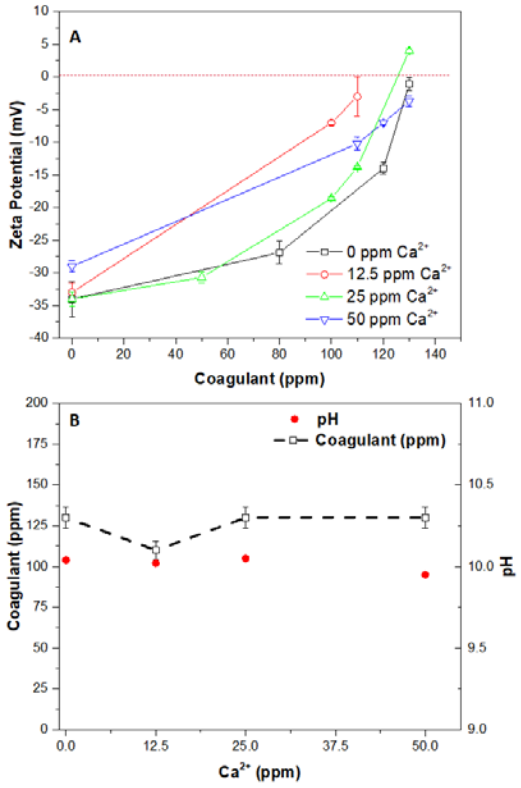

Figure 2.4. (A) the zeta potential of water samples with various concentrations of Ca^{2+} as a function of coagulant dosage at 65 °C, and (B) corresponding optimum coagulant dosage as a function of the concentration of Ca^{2+} determined from the zeta potential measurements.

The effect of dissolved calcium hardness on coagulant dose was studied at different concentrations of CaCl2 from 0 to 50 ppm while all the other constitutents were the same as that of Benchmark water sample. As in the case of $MgCl_2$, the initial zeta potential of the water sample was dependent on the concentration of $CaCl_2$ added in the solution. At 0 ppm calcium ion concentration, the zeta potential was approximately -35 mV and it became less negative as the calcium ion concentration was increased. The optimum coagulant dose did not show any significant difference at 0, 25, and 50 ppm except a small decrease was observed at 12.5 ppm. Based on the t-test analysis, the measured coagulant doses are not statistically different at calcium ion concentration range studied [t = -0.81, df=2, p = 0.05, $t_{critical}$ = 2.92] The plot of coagulant dose at different calcium ion concentration is shown in **Figure 2.4B**. The pH of the system is slightly >10 at Ca2+ concentrations 0, 12.5, and 25 ppm and slightly <10 at 50 ppm Ca2+ concentration.

In the past, several studies have reported the effect of Ca ions on the $CaCO_3$ and $Mg(OH)_2$ surface. In Section 1, we also have reported the effects of excess of calcium ion on $CaCO_3$ particle and found that it shifts the zeta potential of the negatively charged particles to positive. Excess Ca can also bind to HA surface to form molecular complex as well as exchange other metal cations in the precipitated salts through ionic reactions.

2.5. Coagulant dose as a function of the concentration of clay

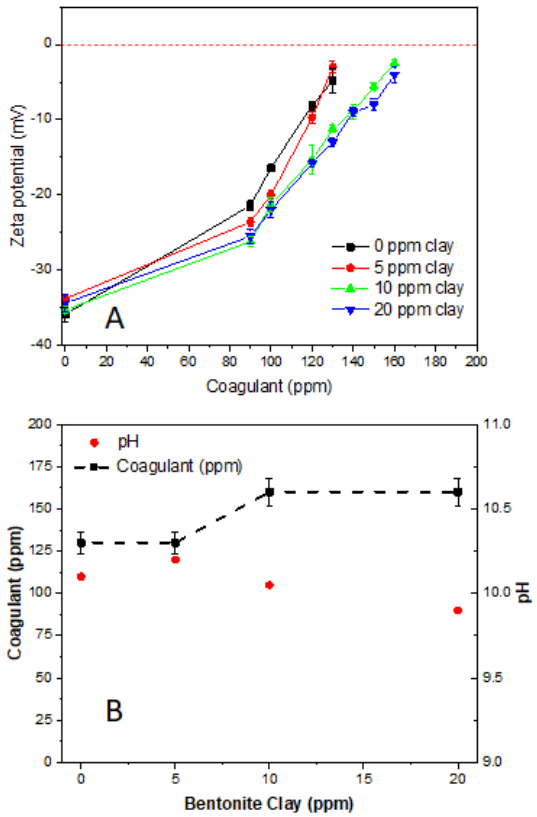

Figure 2.5. (A) the zeta potential of water samples with various concentrations of clay as a function of coagulant dosage at 65 oC, and (B) corresponding optimum coagulant dosage as a function of the concentration of clay determined by the zeta potential measurements.

To improve water reuse, it is possible to recycle tailing water into WLS process. Tailing water has extremely high clay content, athough the stream is typcally minor comparing to PW. The clay concentration in WLS could be elavated up to 25 ppm. To study the effect of clay on the coagulant, bentonite clay ($Al_2O_3{\cdot}SiO_2{\cdot}H_2O$) was added to the water sample at concentrations 0, 5, 10, and 20 ppm. Bentonite has been reported to be negative charged (-30 to -35 mV) from pH of 2 – 12 and behave slightly more negative with increasing pH. **Figure 2.5A** shows that the initial zeta potential of the solution was ~ -35 mV and coagulant was added until the charge neutralization was complete, i.e. the zeta potential was within –5 to +5 mV. From **Figure 2.5B**, it is clear that up to 5 ppm concentration of clay, there was no increase in coagulant dose but at 10 and 20 ppm concentrations, the coagulant dose increased by 30 ppm.
The effect of clay on WLS particles $CaCO_3$ and $Mg(OH)_2$ have been reported in our previous study. As clay itself is known to present negatively charged surface in solution, between the molar ratio of clay to $CaCO_3$

from 0.01 to 0.05, the zeta potential varied from -20 to -25 mV. The zeta potential of clay-$Mg(OH)_2$ mixture in same ratio was between -30 to -35 mV.

2.6. Coagulant dosage as a function of the concentration of $NaHCO_3$

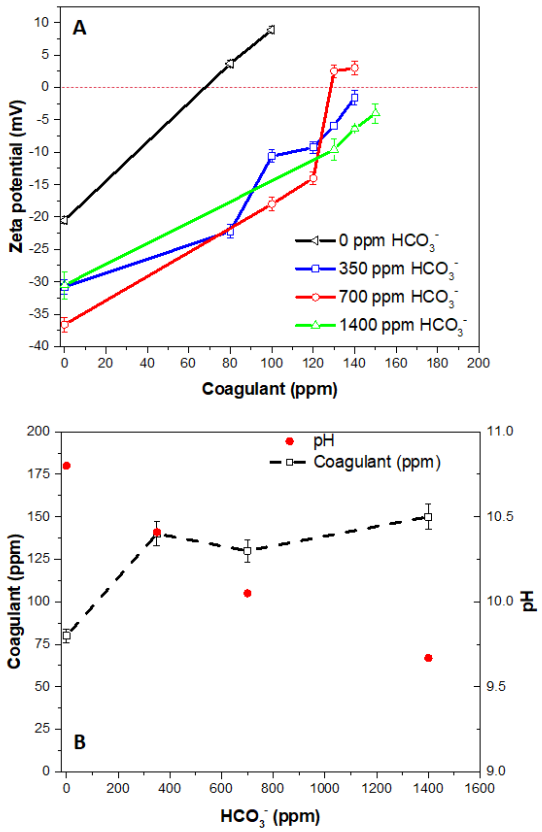

Figure 2.6. (A) the zeta potential of water samples with various concentrations of HCO_3^- as a function of coagulant dosage at 65 °C, and (B) corresponding optimum coagulant dosage as a function of the concentration of HCO_3^- determined from the zeta potential measurements.

Coagulant dose was studied at different bicarbonate alkalinities range from 0 to 1400 ppm in the Benchmark water sample. In Section 1, where the effect of HCO_3^- on $CaCO_3$ and $Mg(OH)_2$ particles was studied, where we found that the dissolved bicarbonate ions introduce negative charge on the particles and zeta potential becomes more negative. Here we saw similar effect of bicarbonate on the initial zeta potentials of the system. The initial zeta potentials were approximately -20, -30, -35 and -30 mV at 0, 350, 700 and 1400 ppm HCO_3^- concentration, respectively (**Figure 2.6A**). The coagulant dosage is also influenced by the initial zeta potential of the system. As shown in **Figure 2.6B**, the coagulant dose is lowest at 0 ppm HCO_3^- concentration. For alkalinity range from 350 to 1400 ppm, the coagulant dose is more or less independent of the HCO_3^- concentration. The t-test analysis also indicates that there is no statistically significant difference between the coagulant doses at these three concentrations [t =2.12, df=1, p=0.05, tcritical = 6.31] The pH decreases from 10.75 to 9.7 with increasing HCO_3^- from 0 to 1400 ppm (**Figure 2.6B**).

2.7. Coagulant dose as a function of the concentration of soda ash (Na_2CO_3)

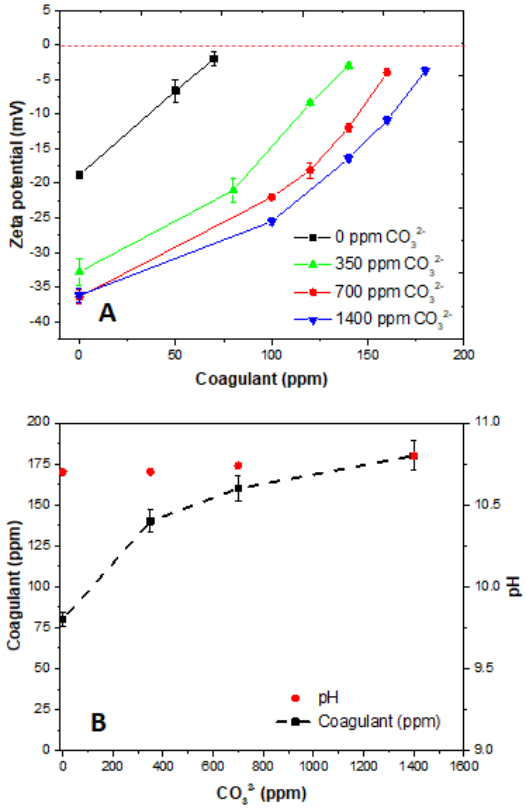

Figure 2.7. (A) the zeta potential of water samples with various concentrations of CO_3^{2-} as a function of coagulant dosage at 65 °C, and (B) corresponding optimum coagulant dosage as a function of the concentration of CO_3^{2-} determined by the zeta potential measurements.

The effect of carbonate alkalinity on the coagulant dose was studied at 0, 350, 700 and 1400 ppm. It is known that presence of carbonate can add negative charge on the particle surface. Our Section 1 study reporting the effect of carbonate ion on the $CaCO_3$ and $Mg(OH)_2$ particles showed that the carbonate ions adsorbed on the particle surface can impart negative charge to these particles. As shown in **Figure 2.7A**, the initial zeta potential of the solution was dependent on the concentration of CO_3^{2-} ions. In absence of CO_3^{2-} ions, the initial zeta potential is less negative (-20 mV) and becomes more negative with increasing concentration of CO_3^{2-} ions.

The pH of the solution did not change significantly with the addition of variable amounts of CO_3^{2-} (**Figure 2.7B**). Additionally, the pH was higher compared to the pH of the solution prepared using HCO_3^- alkalinity. The coagulant dose required to neutralize the particles was plotted against the initial CO_3^{2-} ion concentration which is shown in **Figure 2.7B**. At 0 ppm, the required coagulant dose was 80 ppm. As CO_3^{2-} concentration increased, the coagulant dose also increased. The dose was higher than in case of HCO_3^- ion shown in **Figure 2.6B**. This is because carbonate ion is divalent whereas bicarbonate ion is monovalent. Thus it introduces more negative charge into the solution, thus requiring more coagulant for neutralization.

2.8. Coagulant dosage as a function of the concentration of $Ca(OH)_2$

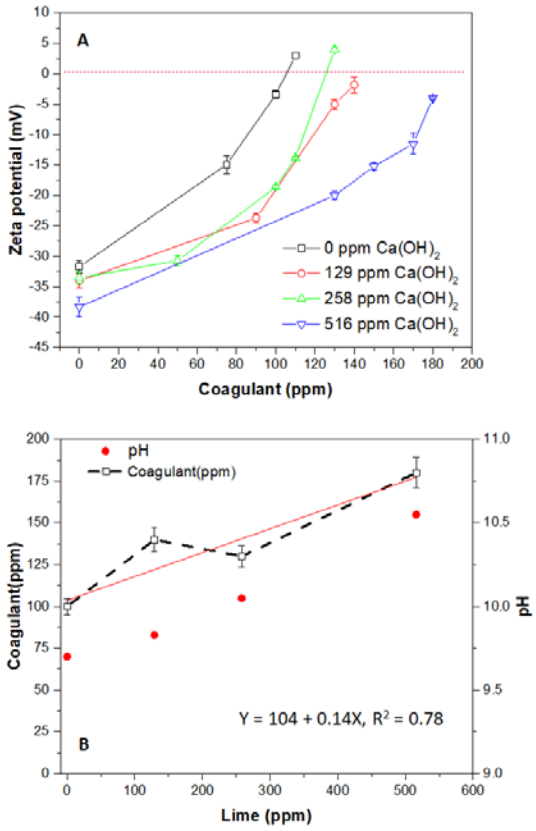

Figure 2.8. (A) the zeta potential of water samples with various concentrations of $Ca(OH)_2$ as a function of coagulant dosage at 65 ^oC, and (B) corresponding optimum coagulant dosage as a function of the concentration of $Ca(OH)_2$ determined from the zeta potential measurements.

Lime is added for the precipitation of dissolved carbonate/bicarbonate as well as precipitation of dissolved Mg. The zeta potential of Benchmark water samples with $Ca(OH)_2$ concentrations of 0 to 516 ppm were measured as a function of coagulant concentration. Before coagulant addition, the zeta potential ranged between -30 and -40 mV as shown in **Figure 2.8A**. The initial zeta potential with 0 ppm $Ca(OH)_2$ was close to -30 mV and became more negative with the increasing $Ca(OH)_2$ addition. At 516 ppm of $Ca(OH)_2$ addition, the zeta potential was close to -40 mV. The increasing negative charge of the water sample with the dose of $Ca(OH)_2$ is a result of the increase in pH at higher dose of $Ca(OH)_2$ which is shown in **Figure 2.8B**. The increased pH also increases the negative charge of the dissolved organic and inorganic particles, thus increasing the required dose of coagulant to attain charge neutralization. Clearly, a steady increase in coagulant dose is observed with the increasing amount of $Ca(OH)_2$, as shown in **Figure 2.8B**. The R2 value also indicated a fairly linear relationship between the coagulant demand and Ca(OH)2 added.

2.9. Coagulant dosage as a function of MgO

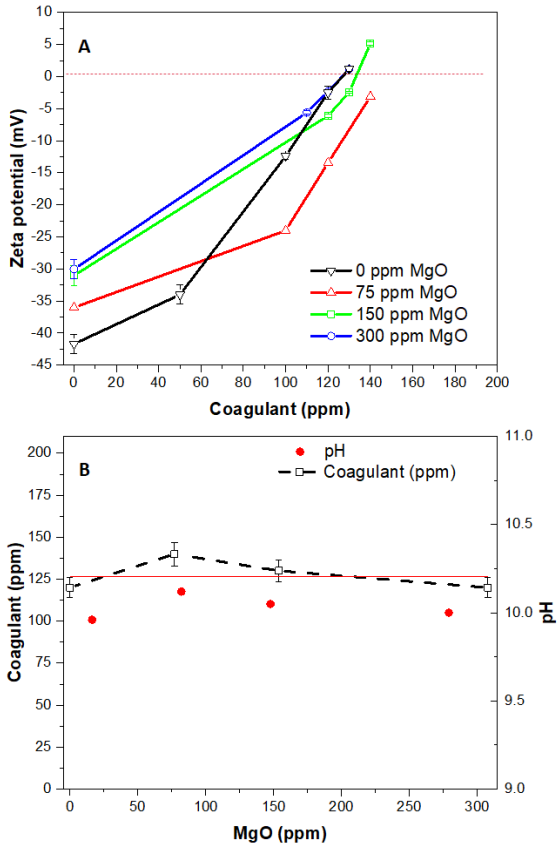

Figure 2.9. (A) the zeta potential of water samples with various concentrations of MgO as a function of coagulant dosage at 65 °C, and (B) corresponding optimum coagulant dosage as a function of the concentraton of MgO determined from the zeta potential measurements.

MgO is used in WLS process to reduce silica level. Using the Benchmark water sample, the effect of MgO on the coagulant dosage was studied at four concentrations of MgO: 0, 75, 150, and 300 ppm. The initial zeta potential of the water sample was approximately -43 mV in absence of MgO; whereas as MgO was added to the system, zeta potential became less negative approaching value of -30 mV at 150 ppm and 300 ppm of MgO (**Figure 2.9A**). The large negative zeta potential in absence of MgO is due to the higher concentration of dissolved silica in the system. As MgO is introduced, silica concentration also decreases and the negative charge also decreases. Accordingly, the coagulant dose also decreased as MgO amount was increased in the system because of the reduction of negatively charged suspended silica particles as shown in **Figure 2.9B**. The pH of the system was approximately 9.8 at 0 ppm MgO and increased to around 10.1 at 75 ppm MgO. At 150 and 300 ppm MgO, the pH was close to 10.

2.10. Determination of silica and HA removal

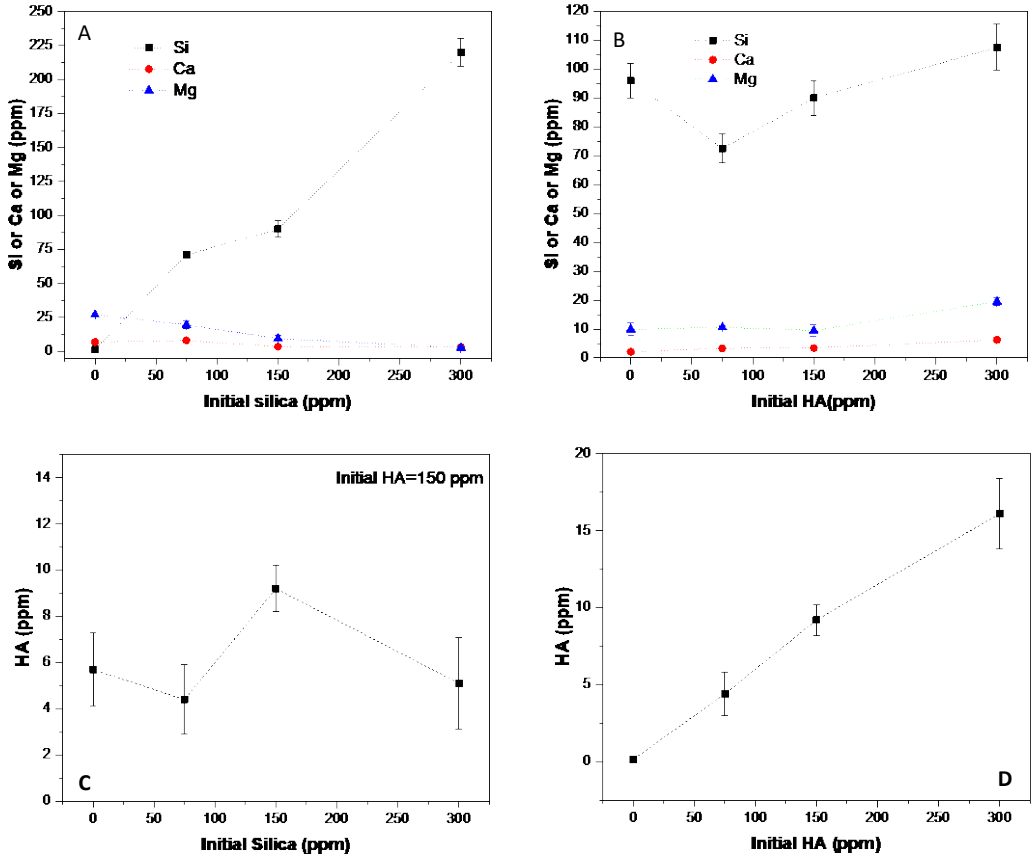

Figure 2.10. ICP measurements of Si, Ca, and Mg in Benchmark water samples with different (A) silica levels (HA = 150 ppm), and (B) HA levels (silica = 150 ppm) after lime softening and coagulation/flocculation process, and corresponding determination of HA by UV-visible spectroscopy at three wavelengths in water samples with different initial (C) silica levels (HA = 150 ppm) (D) HA levels (silica = 150 ppm) .

Ca, Mg, Silica and HA reduction after lime softening and coagulation/flocculation process was studied using Benchmark water samples. **Figure 2.10 A** and **B** show the concentrations of Si, Ca, and Mg measured by ICP-OES as a function of the concentration of silica and HA, respectively. Based on our Section 1 study, precipitation of silica by MgO is most likely to result in the formation of chrysotile ($Mg_3(Si_2O_5)(OH)_4$) followed by sepiolite ($Mg_4Si_6O_{15}(OH)_2{\cdot}6H_2O$) since these are the minerals with highest saturation indexes. At 150 and 300 ppm silica concentration, silica was reduced by 40% and 25% respectively. At 75 ppm, less than 5% silica reduction was found. The MgO concentration was fixed (150 ppm) in all the cases and thus, MgO : silica ratio decreased with increasing silica concentration. The low silica removal at 75 ppm initial silica concentration indicates that other interfering reactions could be hindering the precipitation of silica by MgO. The competing minerals for precipitation reaction are huntie, dolomite, hydromagnesite, etc. Meanwhile, Ca concentration range between 0 and 10 ppm at all Si concentrations. The benchmark concentrations of Ca in water sample are 25 ppm Ca^{2+} and 259 ppm $Ca(OH)_2$. Mg concentration was

approximately 25 ppm at 0 ppm silica concentration and decreased gradually with increasing silica concentration. Note that the measured value is higher than the added $MgCl_2$ solution (Benchmark 15 ppm Mg^{2+}) which indicates that some of the added MgO (Benchmark 154 mg/L) is dissolved to release extra Mg^{2+} ions in the solution.

In another experiment, silica concentration was kept constant (150 ppm) and the HA concentration was varied as shown in **Figure 2.10B**. A silica reduction ranging between 30 to 50% was observed. For 0 to 150 ppm HA, the concentration of Ca was between 0 and 5 ppm and increased slightly at 300 ppm HA. Mg concentration was approximately 10 ppm for 0 to 150 ppm HA and increased to about 20 ppm at 300 ppm HA. The benchmark concentrations of Ca2+ and Ca(OH)2 are 25 ppm and 259 ppm, respectively, while the benchmark concentrations of Mg2+ and MgO are 15 ppm and 154 ppm, respectively. Higher concentrations of Ca and Mg at 300 ppm HA indicates the increase in dissolved Ca and Mg by interaction with the dissolved HA.

The corresponding removal of HA after coagulation was determined by UV-visible spectroscopy. The concentration of HA remaining in the solution was measured by averaging three measurements at 350, 400 and 500 nm.As shown in **Figure 2.10C**, the HA concentration is not directly affected by the starting silica concentration and the average HA concentration after coagulation is between 5 to 10 ppm which corresponds to about 95% removal. HA removal study at different HA concentration is shown in **Figure 2.10D**. As the initial HA concentration is increased from 0 to 300 ppm, the residual HA after coagulation increased as well. However, it is clear that 95% HA is removed during the process.

F. KEY LEARNINGS

In the first part of this project, the electrokinetic properties of $Mg(OH)_2$ and $CaCO_3$ under different conditions such as pH, temperature, CO_2, alkalinity (carbonate and bicarbonate), as well as their binary interactions with other particles such as $CaCO_3$/$Mg(OH)_2$, humic acid, and clay were studied. The zeta potential measurements of the aqueous suspensions of these particles were performed to determine how these particles behave under various experimental conditions. In the second part of this project, organic polycationic compound (quaternary ammonium salt) was used as coagulant to induce coagulation of the suspended particles. The impact of solution chemistry on the coagulant dosage was studied by varying single component of the WLS sample at a time. This study is highly relevant to WLS onsite chemical dosage evaluation and operational controls especially during a WLS effluent off-specification event. The understanding of underlying interaction mechanisms may provide insights on future technology optimization.

The major learnings of this project and their impacts to oil sands industry as well as water and wastewater treatment industry at large can be outlined as follows:

- A lot of parameters relevant to lime softening conditions influence the zeta potential of $CaCO_3$ and $Mg(OH)_2$ particles, among which, pH is the most important parameter. For WLS of oil sands produced water and warm/hot lime softening of industrial wastewater, pH needs to be carefully controlled to adjust the zeta potential of $CaCO_3$ and $Mg(OH)_2$ particles in order to achieve optimum softening performance.

- $CaCO_3$ and $Mg(OH)_2$ particles freshly precipitated during lime softening may behave differently from those preformed including commercially purchased. As recycling a portion of freshly precipitated $CaCO_3$ and $Mg(OH)_2$ particles back into treated stream is not uncommon in WLS of oil sands produced water and warm/hard softening of other industrial wastewater, the operators need to take both freshly precipitated and preformed particles into account.
- Exposing $CaCO_3$ and $Mg(OH)_2$ particles to air changes their zeta potential, this must be taken into consideration, as some industrial softeners are operated in covered vessels with a nitrogen atmosphere to exclude oxygen and CO_2.
- Temperature influences the zeta potential of $CaCO_3$ and $Mg(OH)_2$ particles, for any lime softening operator, bench-scale Jar testing for selecting and optimizing coagulant and flocculant needs to be conducted at the same temperature as the real lime softening process, as bench-scale Jar testing conducted at room temperature will probably provide misleading results for higher temperature lime softening processes. Analytical instruments such as zeta potential analysers can provide useful information on particle charge that may augment the information provided by traditional jar tests. Both the water chemistry including the presence and concentration of different constituents in the source water and added chemicals impacts coagulant dosage. This is very important for SAGD WLS unit operation as during WLS, lime is added for softening and MgO is added to remove silica, which both will influence coagulant dosage.

G. OUTCOMES AND IMPACTS

Project Outcomes and Impacts

WLS is a complex process unit where precipitation, adsorption, coagulation and flocculation take place simultaneously. The outcomes of this project significantly narrowed the knowledge gaps identified above. As demonstrated in project results and key learnings, we were able to explain the charge development of the two common particles present in WLS PW by looking at zeta potential and chemistry modelling. We were also able to qualitatively and quantitatively understand how solution chemistry impacts coagulant dose in a synthetic WLS PW. We expect to develop a new platform where multiple stake holders can work collaboratively to address the existing challenges of water treatment in relation to WLS. This will certainly help to advance the knowledge of the field by generating new data and encourage new practices that will improve the efficiency. The fundamental understanding of particle interactions and factors attributing to coagulant and flocculant dosages narrowed the knowledge gaps where operators have difficulties in determining optimal chemical dosages or adjusting chemical dosages during upset conditions. Ultimately, this study provides valuable data for sustainable water management by improving overall water treatment process in a WLS unit in SAGD facilities.

Program Specific Metrics

The project outcomes will provide a clear understanding of the effects of the reaction conditions on particle surface charge and a logical explanation of the observed behavior, which will in turn transform water treatment process in industrial settings through actionable information. The main findings of this

research will provide practical guideline to optimize WLS process of SAGD produced water and lime softening of industrial wastewater at large. Especially, bench-scale Jar testing for selecting and optimizing coagulant and flocculant for warm and hard lime softening have to be conducted at the temperature for the real softening process, rather than at room temperature, which is mostly the common practice for current industry; the WLS operators need to take both freshly precipitated particles and preformed particles into consideration when designing process of recycling a portion of freshly precipitated particles into treated stream; for any softeners using N_2 blanket to exclude air and CO_2, the impact of exposing to CO_2 on the zeta potential of $CaCO_3$ and $Mg(OH)_2$ particles needs to be considered for process design. The impact of this project is multifaceted. This is of interest to the industry and general public from economic and environmental point of view as industries invest a significant amount of money in water treatment process and the quality and safety of our environmental habitat is dependent on the water released from these industries. It also relates to the ecological impact on wildlife and human health.

Project Specific Metrics

The project supported the training of five highly qualified personnel HQPs (two postdocs, two master graduate candidates and one undergraduate). The results of this project will constitute to the two master theses of the students involved on the project. The data will also be presented at future conferences. The results were already compiled into four manuscripts for publication in relevant peer-reviewed journals. The initial drafts of the manuscripts were reviewed by the involved academic and industrial partners and will be submitted for publication.

H. BENEFITS

Economic: To ensure performance of the process unit, operators tend to overdose chemicals to reduce process risks. Hence economically, it could lead to less expenditures on coagulant and flocculant as a result of optimized dosages. The possession of a better understanding of factors attributing to coagulant and flocculant dosage, operators can quickly adjust to potential process upset conditions which can help maintain the integrity and extend service life of the downstream equipment especially the OTSGs.

Environmental: This objectives and outcomes of this project align with the long-term goal of improving lives of Albertans by creating clean and sustainable environment. The improved process could result in improved boiler feed water quality, hence the OTSGs can run a higher steam quality and generate less blowdown. This could contribute to reduction of wastewater disposal. Improved operation could also lead to better water recycle efficiency and reduced freshwater consumption, which is vital for the sustainability of SAGD operation and oil sands production in Alberta.

Social: The project demonstrated industry's commitment to minimize the impact on the environment by reducing disposal water and increase water recycle efficiency. The joint efforts of the industry and academic community towards resolving problems related to the economy and environment will further strengthen the ties between these communities and promote such collaborations in the future as well. It also helps to familiarize the industrial community to the importance of academic research and prepares young and emerging graduates for careers in industry by bringing them together.

Building Innovation Capacity: This project was beneficial to train several individuals including graduate students and postdoctoral scholars who worked under the guidance of the research professor in well-equipped laboratory. Industrial partners also provided feedbacks at multiple occasions through meetings and presentations. Constant interactions between involved members ensured that the work was progressing smoothly, and scientific and coherent data was being generated. Project team members were trained to use scientific instruments (such as zeta potential analyzer, jar tests, ICP-OES, and so on) throughout the study and chemical modeling softwares (e.g. OLI, VisualMINTEQ) to predict chemical speciation. These skills acquired can be readily applied in most water and wastewater applications where chemical optimization is needed. This experimental setup used can be engaged by many other industries and personnel that are looking for an innovative tool to either improve their water operation or conduct further research into other topics.

I. RECOMMENDATIONS AND NEXT STEPS

Current project focused on advancing the knowledge of the particle interactions and coagulation process in WLS units to provide a better understanding of the process for industries implementing WLS for water treatment. The results of this project are interesting and new questions arise, which need to be addressed in the future. It will be beneficial to pursue further research in the future in following directions:

- Use PW from various SAGD facilities instead of synthetic produced water to conduct further studies as the PW composition may vary from one location to another
- Use additional characterization methods besides zeta potential measurement to understand particle size distribution, morphology, crystal structure and the bonding/adsorption mechanism
- Mimic the industrial sludge recirculation process in the solid contact unit - SAGD WLS unit and understand the impact of sludge recirculation on the performance
- Extend the scope of the water research by taking into consideration the water from other industries such as chemical, textile industries, etc.

J. KNOWLEDGE DISSEMINATION

The knowledge gained from this project has been summarized into four manuscripts for publication in peer-reviewed journals and will also be presented in high-quality conferences. The results will be of interest not only to the industry and academia in the field of SAGD and WLS water treatment system but also to broader water research community. We expect that these reports once available will spark interest of the researchers for further studies. Industries can upgrade and modify their current practices based on these results and continue collaboration with their academic partners to further advance research in the topics relevant to the industry.

K. CONCLUSIONS

In this project, we explored the effects of various experimental parameters such as pH, temperature, aging, dissolved ions on the electrokinetic properties and interactions of the common particles in the SAGD PW. Additionally, the impact of solution chemistry on the polyamine coagulant/flocculant demand of synthetic SAGD PW was studied by varying the concentrations of the components in synthetic PW. Zeta potential measurements provided an idea about the surface charge of the particles in various conditions and chemical modeling using visual MINTEQ software was used to predict chemical speciation. The zeta potentials of $Mg(OH)_2$ and $CaCO_3$ particles vary depending on the pH, temperature, alkalinity, exposure to air, dissolved metal cations. Furthermore, the behavior of preformed particles (i.e. commercially available) may differ drastically compared to the in-situ precipitated particles (i.e. by reaction of their ionic precursors). The observed behavior is well explained by the charge development theory which is described in the literature as well as the possible deposition of new mineral species on the particle surface which introduces new properties. In typical WLS samples, where $Mg(OH)_2$ or $CaCO_3$ particles are present alongside other components such as humic acid, clay, and silica the resulting suspension presents negative zeta potential. Chemical speciation can predict a wide range of minerals under different conditions which help in explaining these properties. Organic polycationic compound (quarternary ammonium salt) are effective coagulants for WLS system. Two important components in WLS system are humic substance and silica which are the major drivers for coagulant demand as indicated by the linear increase of coagulant dose with humic acid and silica concentration. While lime increases the coagulant demand, MgO, $MgCl_2$, and $CaCl_2$ have no obvious effect on coagulant dose. Dissolved bicarbonate or carbonate significantly increases the coagulant dose, and carbonate increases the coagulant demand more than bicarbonate.

These results will be of interest for WLS facilities and affiliated research community. It will assist industries in making WLS process economical thus making environmental mitigation efforts more effective. It will also generate further research interest to understand the particle characteristics and develop efficient treatment methods. This focus of this study was on the effect of solution chemistry on particle charge. In the future, it will be beneficial to study particle properties such as composition, size, morphology, using different analytical techniques which will provide further understanding of the WLS process.